Supporting Information

High-Voltage Deprotonation of Layered-Type Materials as Newly Identified Cause of Electrode Degradation

Junghoon Yang,*[a,b] Sungwon Park,[c] Sungsik Lee,[d] Jungpil Kim,[b] Di Huang,[a] Jihyeon Gim,[e] Eungje Lee,[e] Gilseob Kim,[f] Kyusung Park,[a] Yong-Mook Kang,*[f,g] Eunsu Paek*[c] and Sang-Don Han*[a]

[a] Materials, Chemical, and Computational Science Directorate, National Renewable Energy Laboratory, Golden, CO 80401, USA. E-mail: sang-don.han@nrel.gov.

[b] Carbon and Light Materials Application R&D Group, Korea Institute of Industrial Technology, Jeonju, 54853, Republic of Korea. E-mail: jyang@kitech.re.kr.

[c] Department of Chemical & Biomolecular Engineering, Clarkson University, Potsdam, NY 13699, USA. E-mail: epaek@clarkson.edu.

[d] X-ray Science Division, Argonne National Laboratory, Lemont, IL 60439, USA.

[e] Chemical Sciences and Engineering Division, Argonne National Laboratory, Lemont, IL 60439, USA.

[f] Department of Materials Science and Engineering, Korea University, Seoul, 02841, Republic of Korea. E-mail: dake1234@korea.ac.kr.

[g] KU-KIST Graduate School of Converging Science and Technology, Korea University Seoul, 02841, Republic of Korea. E-mail: dake1234@korea.ac.kr.

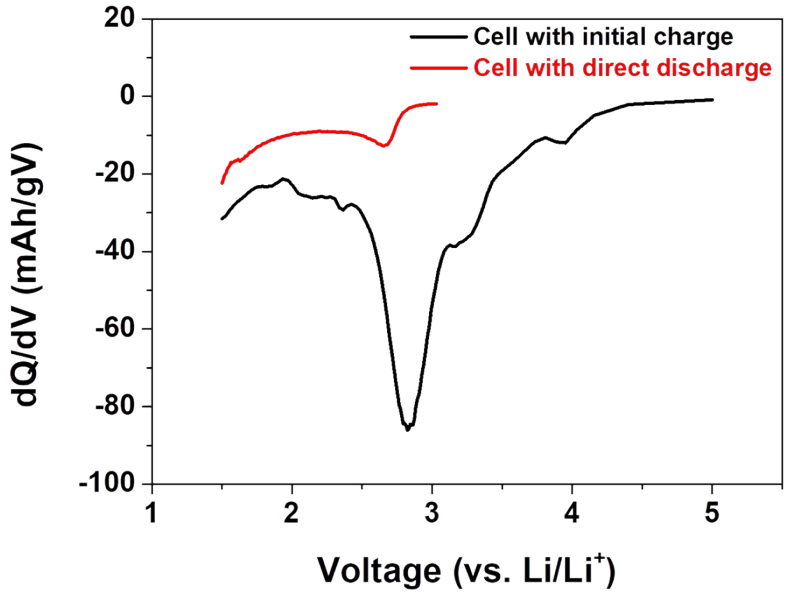

Figure S1. dQ/dV plots of NM-hydroxide obtained from the 1st discharge voltage profile with and without the prior 1st charging process.

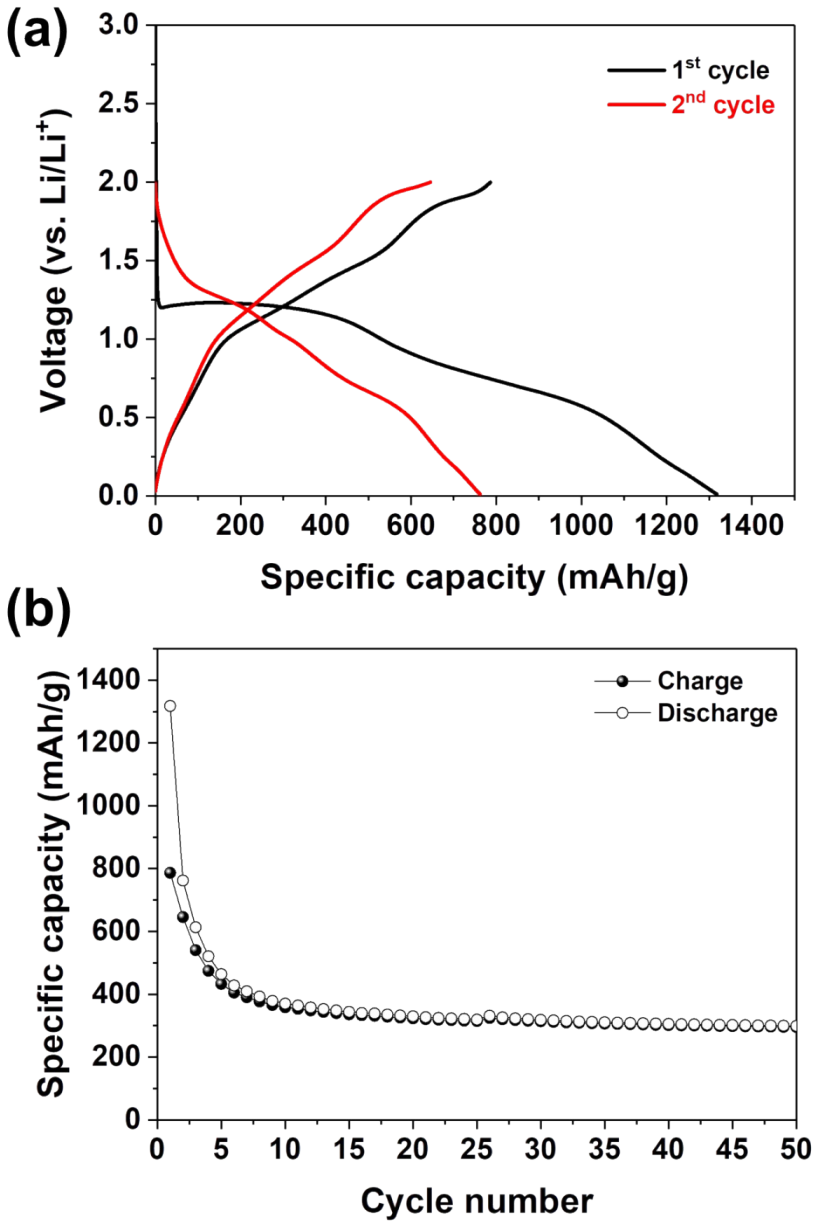

Figure S2. Electrochemical performance of NM-hydroxide electrodes as anode materials: (a) voltage *vs*. specific capacity profile and (b) cycling stability at current density of 20 mAg^{-1} in the voltage range of 0.01-2.0 V.

Figure S2 shows the electrochemical behaviors of NM-hydroxide as an anode material by discharging first from OCV to 0.01V (*vs*. Li/Li^+, hereafter). The plateau observed at ~1.25 V during the 1st discharging is a typical electrochemical signal originated from the conversion reaction of layered hydroxide materials indicating NM-hydroxide can store lithium ions in its structure. In this regard, the gradual increase in discharge capacities of NM-hydroxide based on charging first and then discharging protocol (Figure 2b) demonstrates that during the 1st charging additional reaction may be occurred (in addition to side reactions including electrolyte decomposition and CEI formation) that possibly forms an interstitial site in NM-hydroxide where more lithium ions can be stored.

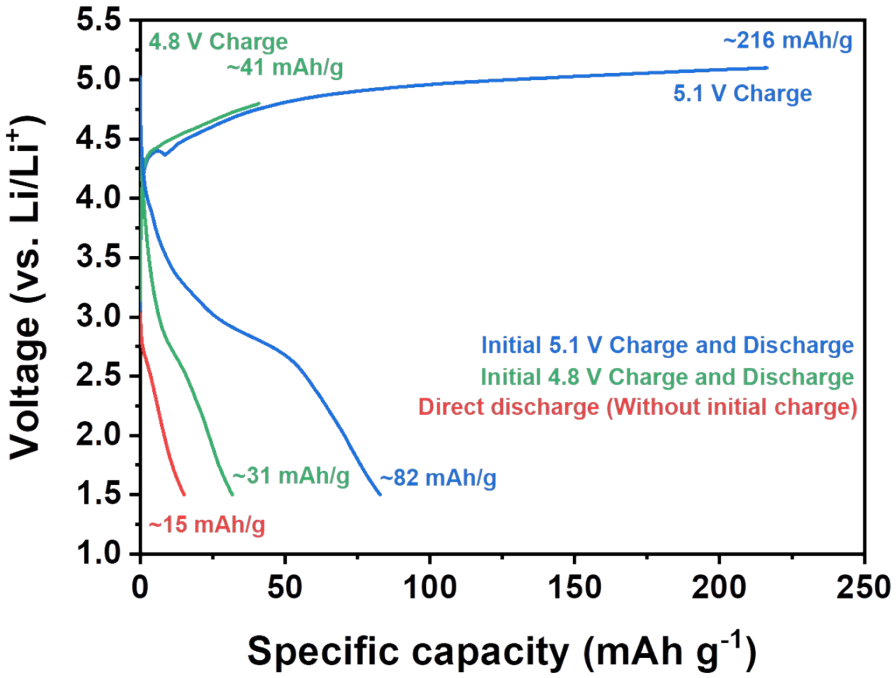

Figure S3. Specific capacity *vs*. voltage profiles of NM-hydroxide for the first cycle based on different electrochemical protocols.

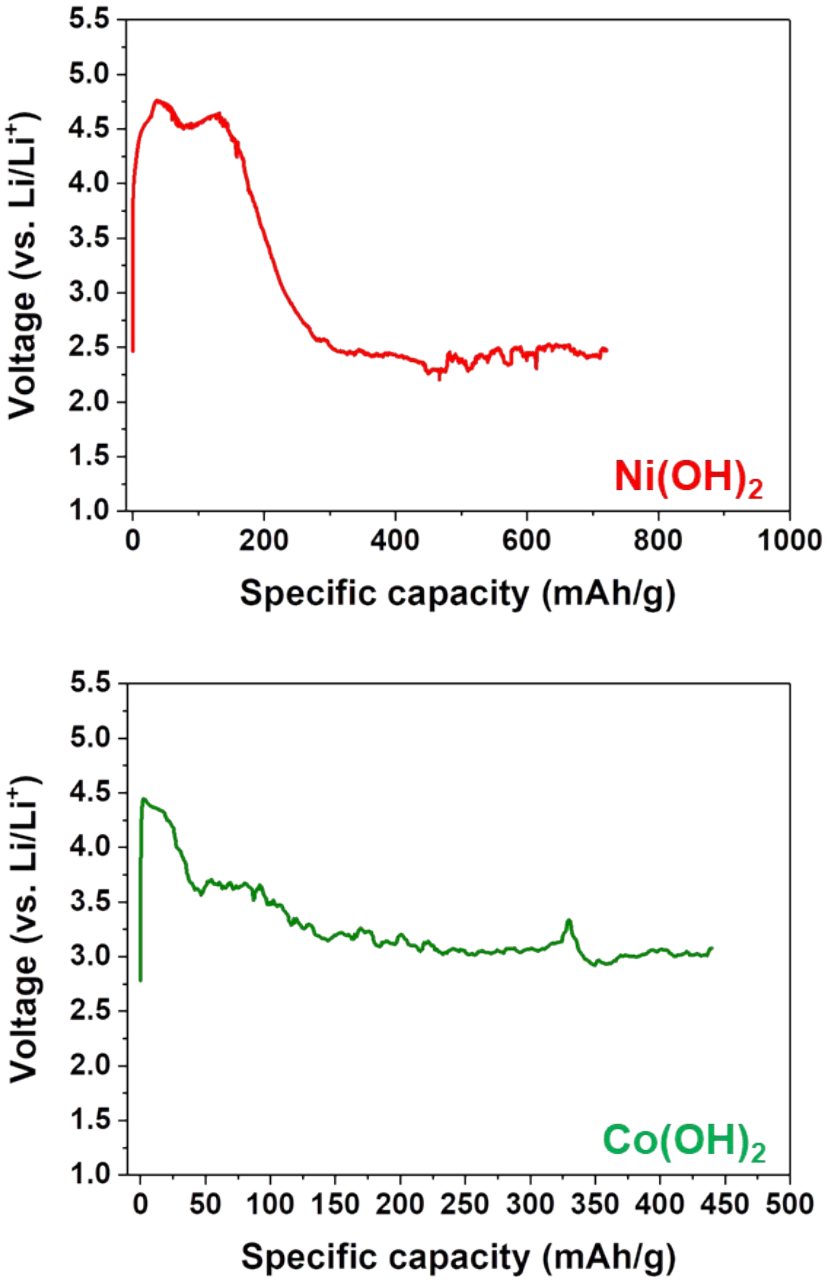

Figure S4. Initial charge profiles of $Ni(OH)_2$ and $Co(OH)_2$ analyzed in the voltage window of 1.5-5.1V (vs. Li/Li^+) at current density of 10 mA/g.

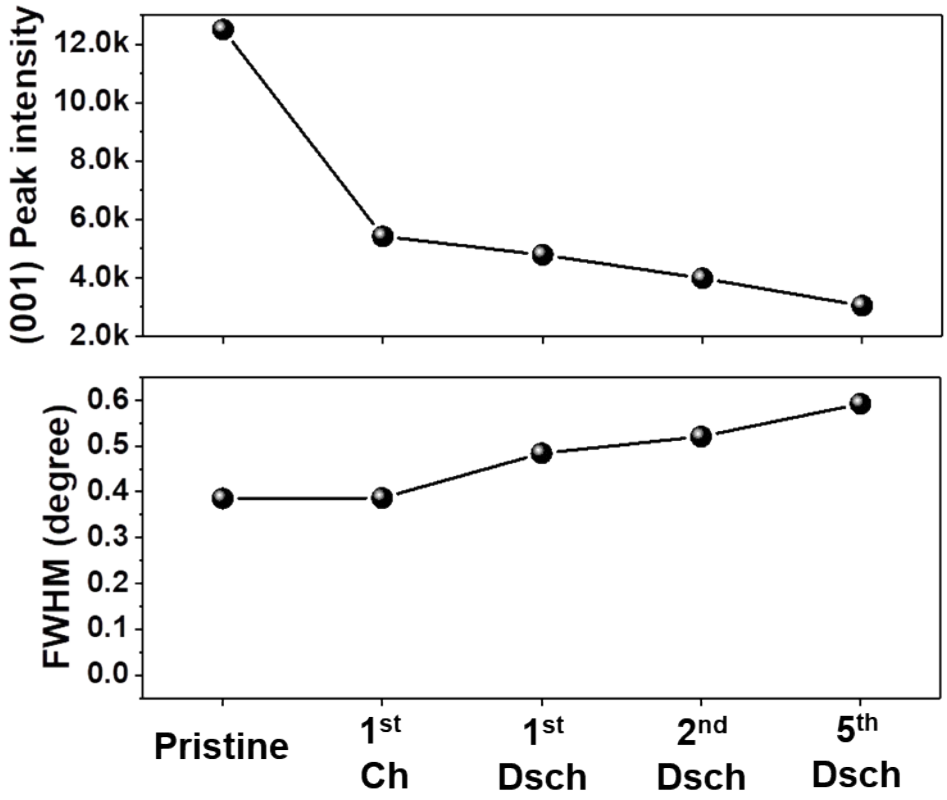

Figure S5. Changes of full width at half maximum (FWHM) and intensity changes of (001) peak obtained from *ex situ* XRD patterns of NM-hydroxide.

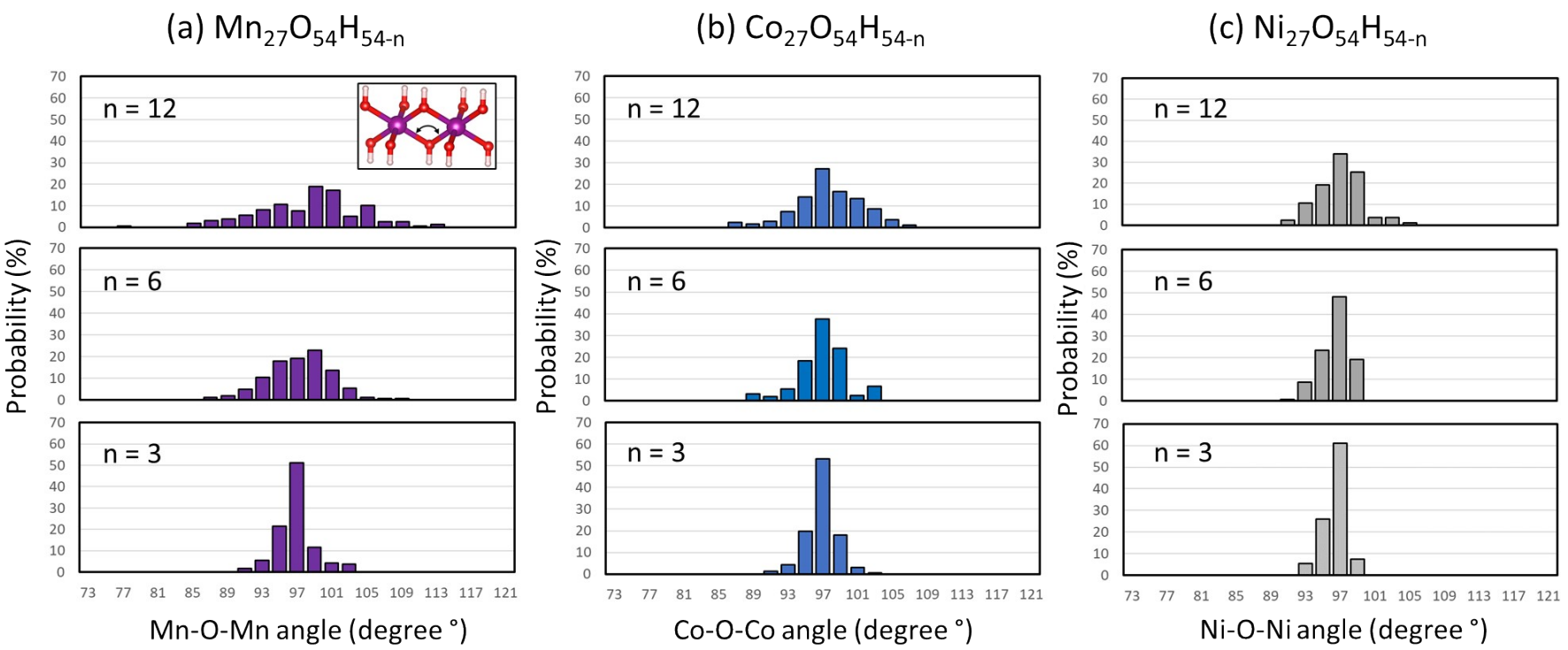

Figure S6. The distributions of (TM-O-TM) angles for (a) $Mn_{27}O_{54}H_{54-n}$, (b) $Co_{27}O_{54}H_{54-n}$ and (c) $Ni_{27}O_{54}H_{54-n}$ with various dehydrogenation levels (n = 3, 6 and 12).

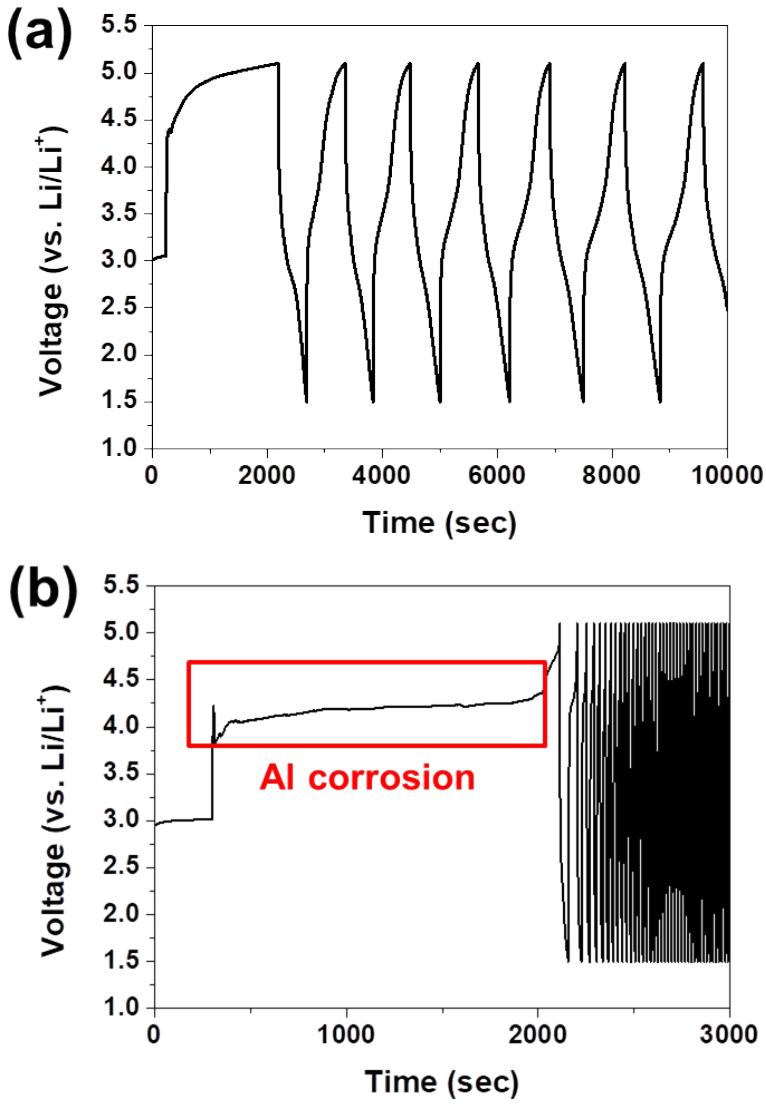

Figure S7. Time *vs*. voltage profiles of NM-hydroxide in (a) Gen2 and (b) LiTFSI-EC/EMC electrolytes.

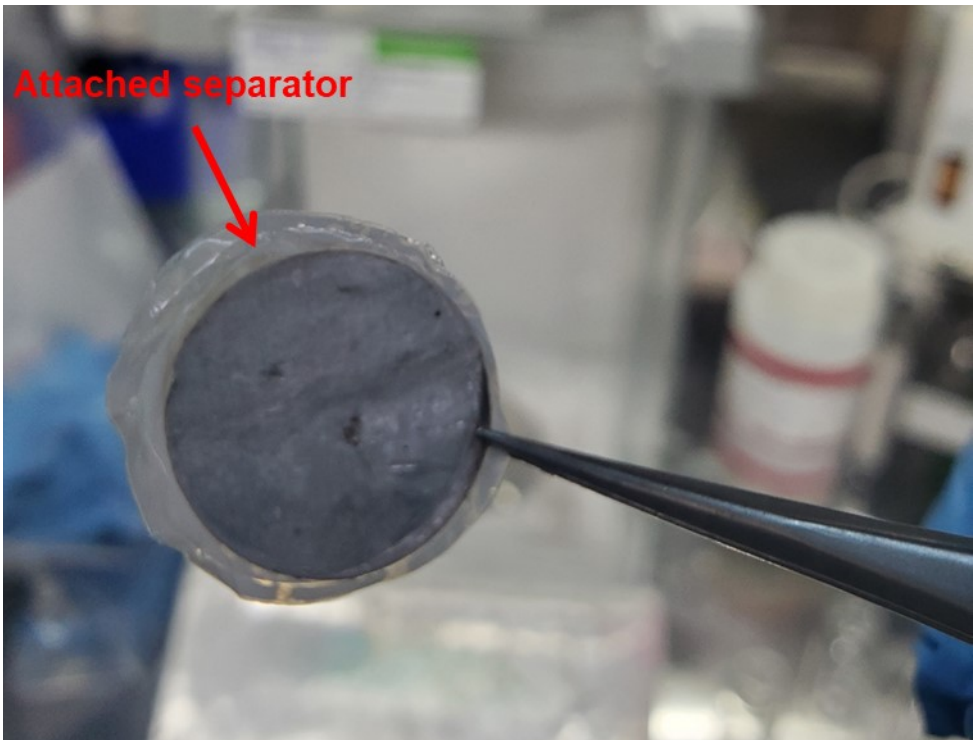

Figure S8. Photo image of the attached separator on the cycled Li metal anode in the Gen2 electrolyte.

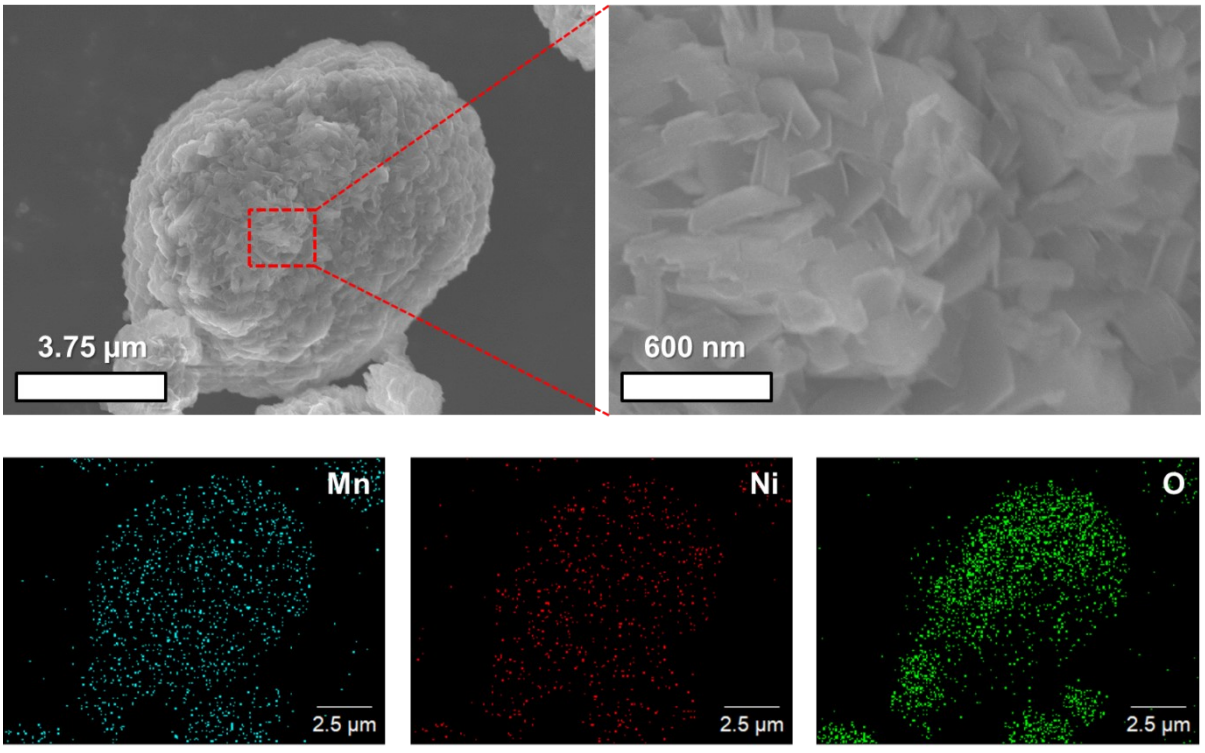

Figure S9. SEM image of a NM-hydroxide particle and corresponding EDS elemental mapping for Mn, Ni and O.

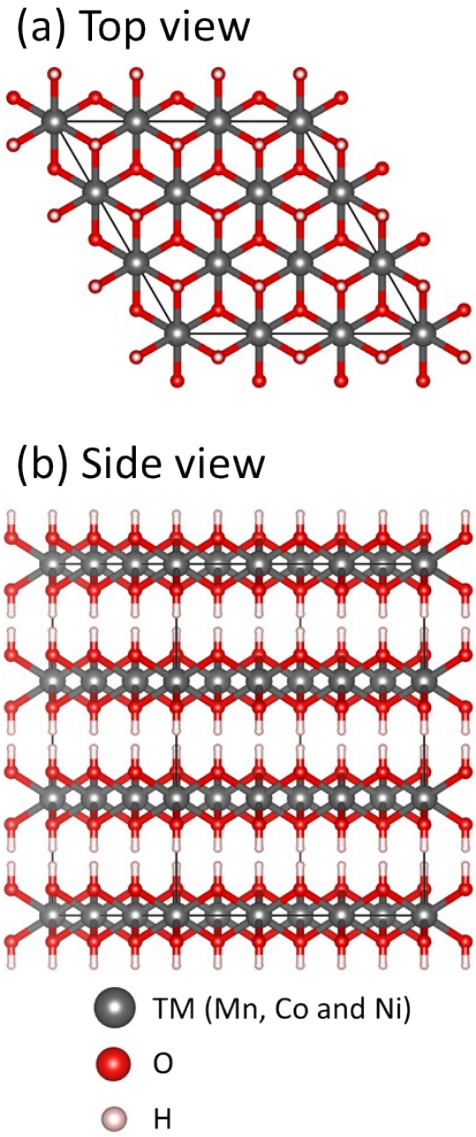

Figure S10. (a) top and (b) side view of the 3 × 3 × 3 $TM(OH)_2$ supercell (TM = Mn, Co and Ni).